

# Structure and catalytic processes of N-containing species on Rh(111) from first principles

J.M. Ricart<sup>a,\*</sup>, F. Ample<sup>a</sup>, A. Clotet<sup>a</sup>, D. Curulla<sup>b</sup>, J.W. (Hans) Niemantsverdriet<sup>b</sup>, J.F. Paul<sup>c</sup>,  
J. Pérez-Ramírez<sup>d</sup>

<sup>a</sup> *Departament de Química Física i Inorgànica, Universitat Rovira i Virgili, C/Marcel·lí Domingo s/n, E-43007, Tarragona, Spain*

<sup>b</sup> *Schuit Institute of Catalysis, Eindhoven University of Technology, PO Box 513, 5600 MB, Eindhoven, The Netherlands*

<sup>c</sup> *Laboratoire de Catalyse de Lille, USTL/CNRS, F-59655, Villeneuve d'Ascq cedex, France*

<sup>d</sup> *Yara Technology Centre Porsgrunn, PO Box 2560, N-3908, Porsgrunn, Norway*

Received 15 December 2004; revised 3 March 2005; accepted 4 March 2005

Available online 8 April 2005

## Abstract

Density functional theory has been used to gain molecular understanding of various catalytic processes involving N species on Rh(111). These include CN, N<sub>2</sub>, and HCN formation and N<sub>2</sub>O decomposition. Our calculations substantiate the conclusion that, starting from chemisorbed C and N atomic species, CN formation is preferred over N<sub>2</sub> formation, because of the lower activation energy of the former process (1.73 vs. 2.10 eV). HCN formation has been studied starting from adsorbed CH and N species, with a computed activation barrier of 1.35 eV. The process of binding CH to N is more favorable than recombination of C and N atoms into CN followed by hydrogenation. Concerning the adsorption and dissociation of N<sub>2</sub>O on Rh, two pathways have been investigated, leading to N<sub>2</sub> or NO. From thermodynamic considerations, N<sub>2</sub> can be concluded to be the preferred product resulting from N<sub>2</sub>O dissociation. Our results also support the participation of N<sub>2</sub>O as a reaction intermediate during reduction of nitric oxide to nitrogen over Rh surfaces by reaction of adsorbed NO and N atoms.

© 2005 Elsevier Inc. All rights reserved.

**Keywords:** First principles; DFT; Chemisorption; Catalysis; Rhodium; Rh(111); N species; CN; HCN; N<sub>2</sub>O

## 1. Introduction

Heterogeneous catalysis is the basis for the majority of chemical production processes in industry. In the last 10 to 20 years, significant advances have been made in acquiring a deeper mechanistic understanding of catalytic processes by the application of novel surface science techniques with model surfaces under ultrahigh-vacuum conditions [1–3] and theoretical approaches based on quantum chemical principles [4–8]. Ab initio theoretical methods have now reached the point where molecular structures and adsorbed species on solid surfaces are predicted with accuracy comparable to that of the most sophisticated experimental methodolo-

gies. This provides information about the nature of the active sites, adsorbate structure, adsorption and activation energies, and reaction paths, which is essential information for reactor design and process scale-up. Computational approaches can be of significant help in the rational catalyst design of new and well-established processes. This is excellently exemplified by recent work from Jacobsen et al. [9], who accomplished the computational development of novel Co–Mo alloys for ammonia synthesis displaying higher activities than the typical Fe- and Ru-based catalysts.

In this paper we apply density functional theory (DFT) calculations to periodic models to gain a mechanistic insight into various catalytic processes involving N-containing species on rhodium surfaces. Cases subjected to study include the structure and formation of CN, N<sub>2</sub>, and HCN adsorbed species and the adsorption and dissociation reactivity of N<sub>2</sub>O on Rh(111) and its involvement as a reaction in-

\* Corresponding author. Fax: +34 977559563.

E-mail address: [josep.ricart@urv.net](mailto:josep.ricart@urv.net) (J.M. Ricart).

intermediate in de-NO<sub>x</sub> reactions. The mechanisms of these particular processes have not been fully resolved yet, particularly with regard to the aspects mentioned below.

### 1.1. CN and HCN formation

HCN is typically found as an unwanted product in the reduction of nitric oxide (NO) by hydrocarbons on rhodium catalysts in car exhaust purification [10]. This process likely involves the presence of surface cyanide (CN) species as a reaction intermediate. CN can be formed by the recombination of adsorbed C and N atoms [10–14]. Van Hardeveld et al. studied the reaction of NO [10] or atomic nitrogen atoms [11] with ethylene (C<sub>2</sub>H<sub>4</sub>) on Rh(111). The main product of the reaction at low ethylene doses was N<sub>2</sub>. However, the selectivity of the reaction for HCN increased with increasing ethylene exposure, thus suggesting that cyanide formation occurs via the reaction between adsorbed N atoms with atomic adsorbed C atoms or hydrocarbon fragments. Moreover, it was reported that whereas N<sub>2</sub> desorbs normally between 500 and 750 K from Rh(111), desorption was retarded at higher temperatures (650–850 K) after exposure to ethylene. This was attributed to CN formation, and, in the absence of surface hydrogen, these CN groups were found to be stable up to ~ 700 K. Herceg and Trenary [12], investigating the CH<sub>3</sub>I + NH<sub>3</sub> reaction on Pt(111), also concluded that the C–N coupling occurs via interaction of adsorbed C and N atoms.

### 1.2. Processes involving N<sub>2</sub>O

Nitrous oxide (N<sub>2</sub>O) is a harmful gas in our environment, contributing to ozone layer depletion and the greenhouse effect. The major industrial source of N<sub>2</sub>O is the production of nitric acid. Other sources are production plants that produce adipic acid, caprolactam, glyoxal, and acrylonitrile, and, in general, processes using HNO<sub>3</sub> as the oxidant or involving oxidation of ammonia [15,16]. Direct catalytic decomposition of N<sub>2</sub>O into N<sub>2</sub> and O<sub>2</sub> represents an attractive and cost-effective technology for reducing emissions in tail gases [16]. Rh-based catalysts on different supports, including single and mixed oxides and zeolites, have been considered the most active systems for direct N<sub>2</sub>O decomposition at low temperatures. Although there are some theoretical studies that deal with N<sub>2</sub>O adsorption to metal surfaces, including Pd, Cu, Ni, Pt, and Rh [17–23], the mechanisms for N<sub>2</sub>O formation and dissociation are not yet fully understood.

In addition, the occurrence of N<sub>2</sub>O as a possible reaction intermediate in the mechanism of NO reduction to N<sub>2</sub> over Rh-based catalysts is controversial and remains unsolved [24]. An accepted description is that after NO dissociation the resulting N surface atoms recombine, yielding N<sub>2</sub> [25]. Whereas Belton et al. [26] discarded the involvement of N<sub>2</sub>O in the NO + N reaction over Rh(111), Zaera and Gopinath [27,28] postulated that N<sub>2</sub>O is an intermedi-

ate during the reduction of NO with CO to N<sub>2</sub> over Rh(111). Ma et al. [29] indicate that N<sub>2</sub> is produced via N<sub>2</sub>O as an intermediate species at T ≤ ~ 600 K in the NO + CO reaction on Pd(110), although at higher temperatures the associative desorption of nitrogen atoms prevailed. It has also been shown that molecular oxygen is produced via both interaction of N<sub>2</sub>O with adsorbed oxygen species formed from N<sub>2</sub>O and recombination of adsorbed oxygen species on the surface over a Pt–Rh alloy gauze catalyst [30]. On this basis competitive decomposition of adsorbed N<sub>2</sub>O into N<sub>2</sub> or NO can be envisaged, although the formation of NO upon interaction of N<sub>2</sub>O with catalytic surfaces in steady-state or transient experiments, where N<sub>2</sub> and O<sub>2</sub> are the decomposition products, has not been reported in the literature.

## 2. Computational details

The Rh(111) surface was modeled by a three-metal layer periodic slab with seven vacuum layers and a  $p(3 \times 3)$  unit cell for the study of CN and HCN. To study the reactivity of N<sub>2</sub>O we considered five metal layers and a  $p(2 \times 2)$  unit cell. The positions of the Rh atoms were taken from the optimized value for the bulk lattice parameter of 3.849 Å, which is very close to the experimentally determined value of 3.803 Å. In the case of CN and HCN, the rhodium atoms of the first surface layer were allowed to relax, while the other two layers were frozen. In the case of N<sub>2</sub>O the three upper layers were relaxed, although the relaxation of the second layer was smaller than ~ 0.2%

The calculations were performed in the framework of density functional theory, with the use of periodic models and the Vienna Ab Initio Simulation Package (VASP) [31–33]. The exchange-correlation functional used was the gradient-corrected form proposed by Perdew and Wang (PW91) [34]. The electron–ion interaction is described by ultrasoft pseudopotentials [35] with a cutoff energy for the plane-wave expansion of 400 eV. Brillouin-zone integration was performed with grids of  $6 \times 6 \times 1$  Monkhorst-Pack [36] special k points. The optimization of the atomic positions is performed via a conjugate gradient minimization of the total energy using the Hellmann–Feynman forces on the atoms. We used the climbing-image nudged-elastic-band method (CI-NEB) [37] to obtain minimum energy pathways and transition-state structures.

The adsorption energies ( $E_{\text{ads}}$ ) were calculated according to  $E_{\text{ads}} = E_{\text{mol/sub}} - (E_{\text{mol}} + E_{\text{sub}})$ , where  $E_{\text{sub}}$  is the empty substrate energy,  $E_{\text{mol}}$  is the energy of the molecule in the gas phase, and  $E_{\text{mol/sub}}$  is the energy of the adsorbed molecule. A negative value of  $E_{\text{ads}}$  indicates an exothermic process. Since the CN radical is not stable in the gas phase, the adsorption energy is referenced to  $\frac{1}{2}$  C<sub>2</sub>N<sub>2</sub>.

### 3. Results and discussion

#### 3.1. CN and HCN production

##### 3.1.1. CN, HCN, and N<sub>2</sub> adsorption modes

First we investigated the adsorption of carbon and nitrogen atoms on the Rh(111) surface. Carbon and nitrogen have a similar energy profile; the preferred adsorption site is the hcp threefold hollow site, with an adsorption energy of  $-8.12$  eV for atomic carbon and  $-5.40$  eV for atomic nitrogen, with respect to the atoms in the gas phase. Subsequently, the binding of CN species to the surface was explored. The most stable CN adsorption mode molecule is perpendicular to the fcc site with an adsorption energy of  $-4.02$  eV with respect to the CN radical in the gas phase, which corresponds to  $-0.85$  eV with respect to  $\frac{1}{2}$  C<sub>2</sub>N<sub>2</sub>. The C–N distance is  $1.20$  Å, only slightly larger than the value for the gas-phase CN radical ( $1.17$  Å). However, as

shown in Fig. 1, other modes (on top, bridge, hcp, or even bidentate structures are within a narrow range of energy between  $-0.61$  and  $-0.85$  eV, with respect to gas-phase cyanogen). This adsorption mode is different on surfaces such as Pt(111) [38,39], where the most stable configuration is the top site, with an adsorption energy of  $-3.64$  eV with respect to CN or  $-0.47$  eV with respect to  $\frac{1}{2}$  C<sub>2</sub>N<sub>2</sub>. As in the present study, several adsorption modes appeared to be feasible in a narrow range of adsorption energies on Pt(111). Similar results were also reported for CN on Ni [40] or Au [41] surfaces. The adsorption of molecular nitrogen on the surface is stable only on top sites with an adsorption energy of  $-0.50$  eV, with the N–N bond perpendicular to the metal surface.

Fig. 2 shows the structures and energetic levels for the more stable stationary points of HCN adsorbed to Rh(111). The most stable adsorption mode is on the hcp site via the C atom. The adsorption energy with respect to HCN in the gas

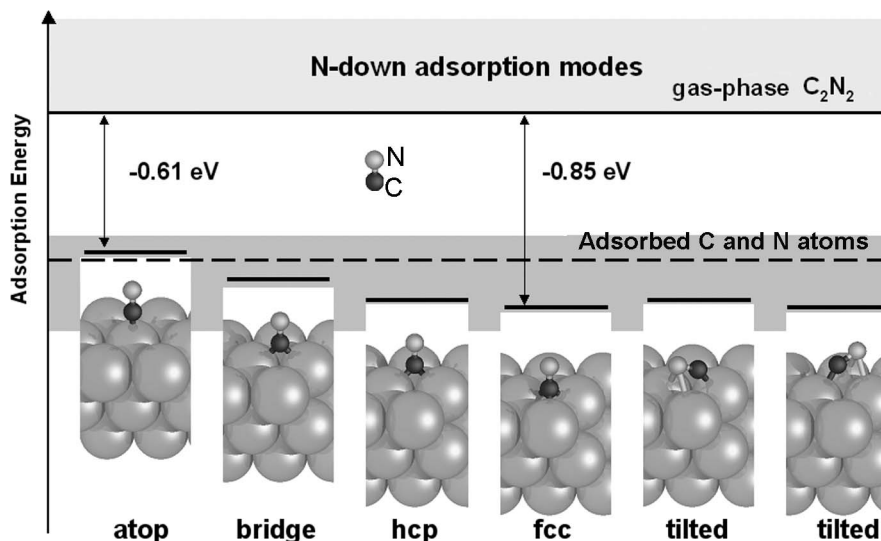


Fig. 1. Adsorption of CN on Rh(111). Only the modes with the C-atom bound to the surface are shown: top, bridge, hcp, fcc, and two tilted modes. The adsorption energy of the co-adsorbed C + N atoms is represented by the thick dash-line.

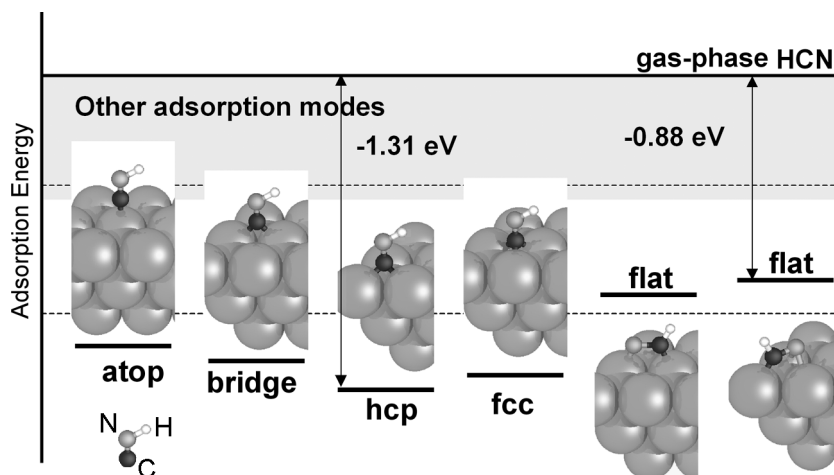


Fig. 2. Adsorption of HCN on Rh(111); only the modes in which HCN binds through the carbon atom and two tilted modes are shown.

phase is  $-1.31$  eV. The C–N distance is  $1.24$  Å in the adsorbate, longer than for the gas-phase molecule ( $1.17$  Å), with an H–C–N angle of  $124^\circ$ . We have also explored the different structures (not shown in Fig. 2) bound to the surface via N; these are always less stable than those bound through the C atom of HCN. Finally, we located two  $\eta_2$  flat modes with the H atom linked to C or N, which are nearly degenerate in energy.

### 3.1.2. Selectivity for CN and $N_2$

Fig. 3 shows a pathway for the formation of a CN species bound through C from the atoms, in which the N atom moves toward the C atom. The calculated activation energy for cyanide formation, from its constituent atoms adsorbed at threefold hcp hollow sites, is  $1.73$  eV, whereas the CN decomposition has a somewhat higher activation energy of  $1.89$  eV. Accordingly, the exothermicity amounts to only  $-0.16$  eV. The structure of the transition state, where C is at the hollow site and N is near the bridge site, agrees with the results from Michaelides and Hu for the same reaction on Pt(111) [42], although the barrier on Pt(111) was significantly lower ( $0.82$  eV). This provides additional support to the hypothesis of Michaelides and Hu that in this type of reaction on metallic (111) surfaces, the adsorbate with a lower valence is activated over the bridge site. An alternative minimum-energy pathway where the C atom moves to N to form adsorbed CN also via C has been calculated as well. The energy barrier for this path is  $1.79$  eV, a value only slightly higher than the previous one.

The formation of  $N_2$  follows similar trends, but, in this case, the transition state is formed by two N atoms in hollow sites. The path leads to  $N_2$  adsorbed to a hollow site, which subsequently may shift to the top position, with an additional energy gain of  $-0.6$  eV. Alternatively,  $N_2$  may desorb. The exothermicity for the recombination of adsorbed nitrogen atoms is  $-0.35$  eV, slightly higher than for CN formation, but the calculated activation energy is  $2.10$  eV, which is larger than that for CN formation. This explains the preferential formation of adsorbed CN over  $N_2$  as observed in a temperature-programmed experiment [11]. Moreover,

the stability of the CN species on Rh(111) is closely related to the fact that there are several adsorption modes for CN within a narrow range of adsorption energies. Hence, the CN species is likely to have a high mobility on the surface, and therefore dissociation of CN through an immobilized or tight transition state [5] would mean a considerable loss of entropy. As this is by no means compensated for energetically, dissociation of CN is unfavorable and therefore possible only at elevated temperatures, as indeed observed by Van Hardeveld et al. [10,11].

### 3.1.3. Formation of HCN

A minimum-energy pathway for HCN formation has been obtained, starting from adsorbed CH and N species and concluding with a flat adsorbed HCN (Fig. 4). The most favorable position for the CH species is the hcp hollow site, with a formation energy of  $-0.45$  eV with respect to adsorbed H and C atoms. In the pathway, the N atom moves toward the CH species. The energy barriers for the formation of HCN and decomposition are  $1.35$  and  $1.05$  eV, respectively. The transition state is above the energy for the free molecule. If we start from C, N, and H adsorbed to Rh(111) and disregard the presence of NH on the surface [11], two possibilities can be conceived for HCN formation: (a) CH formation and reaction with N or (b) CN formation and hydrogenation [11]. As we have seen, the barrier for the HCN formation from CH and N ( $1.35$  eV) is smaller than that for CN formation ( $1.73$  eV). On the other hand, the energetic barrier for CH formation is predicted to be on the order of  $\sim 0.5$  eV [43], much lower than that for CN formation. Thus, the path that binds adsorbed CH and N is energetically favored over formation of CN and its hydrogenation. This supports TPD results reported by Herceg and Trenary [12]. They found that the C–N coupling cannot occur directly by reaction of  $CH_3$  and  $NH_3$  and, accordingly, must proceed through their dissociation products. However, the same authors also observed that in the absence of  $CH_x$  and  $NH_y$  species the C–N coupling takes place directly from adsorbed C and N atoms. Adsorbed CH is predominant in the decomposition of hydrocarbons like ethylene [1]. There-

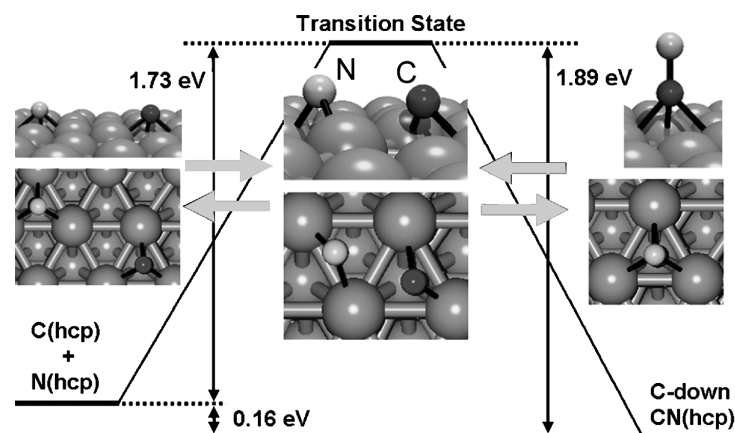


Fig. 3. Reaction and transition state geometry for CN formation from adsorbed C and N atoms on Rh(111).

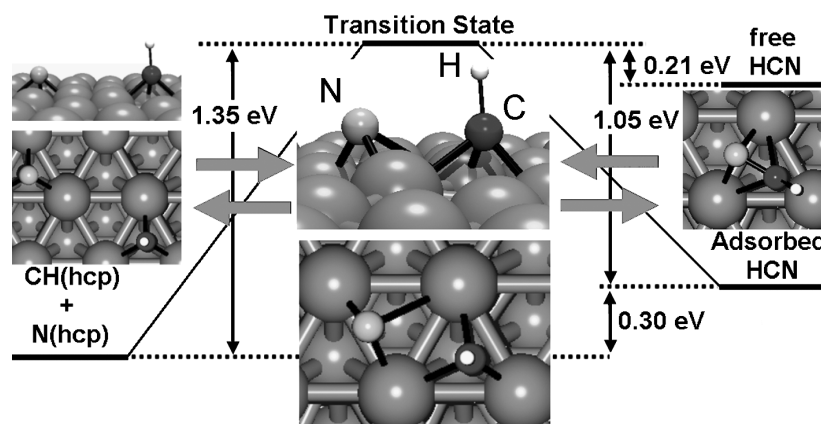


Fig. 4. Reaction and transition state geometry for HCN formation from adsorbed CH + N on Rh(111).

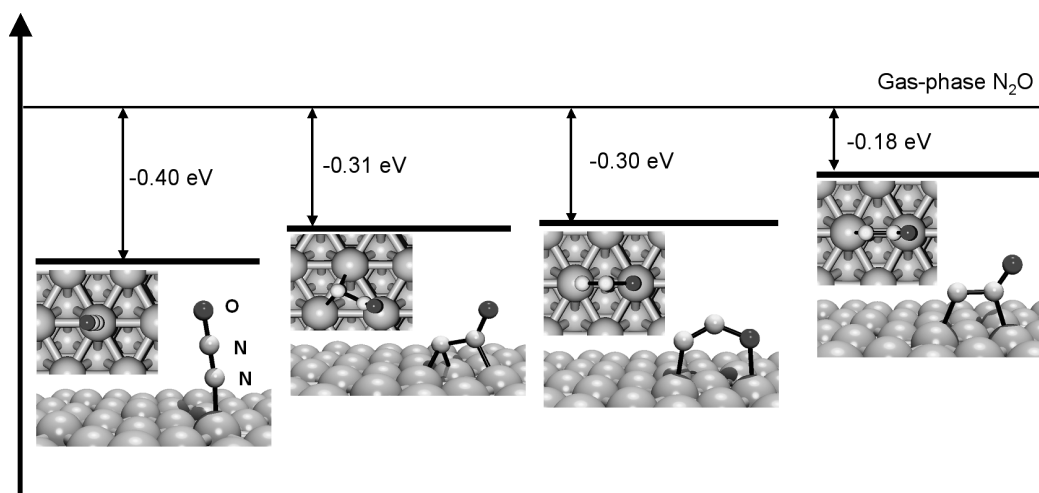


Fig. 5. Structures of the most stable modes of adsorbed N<sub>2</sub>O on Rh(111).

fore, the formation of HCN via the CH fragments is plausible and energetically favored and in agreement with experimental findings.

### 3.2. N<sub>2</sub>O decomposition

#### 3.2.1. N<sub>2</sub>O adsorption

We explored the various adsorption modes of N<sub>2</sub>O, including two  $\eta_1$  modes (by N<sub>t</sub> or O) and three  $\eta_2$  modes (N<sub>t</sub>N<sub>c</sub>, N<sub>t</sub>O, and N<sub>c</sub>O, where t stands for terminal and c for central). The most stable system corresponds to adsorption through the terminal N<sub>t</sub> atom on top of one Rh atom, with an adsorption energy of  $-0.40$  eV (Fig. 5). The molecule is tilted slightly (about  $7^\circ$ ), but the potential energy surface is very flat as a function of the tilting angle. The present results are similar to the calculations by Kokalj et al. [17,18] for N<sub>2</sub>O on Pd(110). The adsorbed N<sub>2</sub>O molecule undergoes hardly any distortion ( $d_{N-N} = 1.15$  Å and  $d_{N-O} = 1.21$  Å) as compared with the calculated N–N and N–O distances in the free molecule, 1.15 and 1.21 Å, respectively, which indeed are in good agreement with the experimentally determined values (1.127 Å for  $d_{N-N}$  and 1.185 Å for  $d_{N-O}$ ) [44].

Interaction of N<sub>2</sub>O through the terminal N<sub>t</sub> atom with other positions on the surface is negligible ( $-0.05$  eV <  $E_{\text{ads}}$  < 0.05 eV), indicating that the displacement of the adsorbed N<sub>2</sub>O molecule on the surface will lead to its spontaneous desorption.

Other stable structures of adsorbed N<sub>2</sub>O originate from interactions between the two N atoms and the surface. The most stable configuration occurs when the N<sub>t</sub> atom is in bridging position and the N<sub>c</sub> atom is in top position, with an adsorption energy of  $-0.31$  eV. In this case, the molecule is distorted; the N–N–O angle is  $123^\circ$ . The variation of the N–N distance is important (1.35 Å) as compared with that in gas-phase N<sub>2</sub>O (1.15 Å). In contrast, the N–O distance remains very similar (1.22 Å). Hence, as the N–N bond is largely activated whereas the N–O bond is not distorted, this adsorption mode is considered a suitable starting point for the dissociation of the N<sub>2</sub>O molecule into adsorbed NO and N species.

The adsorption via the two terminal atoms (N<sub>t</sub> and O) is also stable. An adsorption energy of  $-0.30$  eV is computed when the two terminal atoms are in top position. Once again, the geometry of the adsorbed molecule is very different from

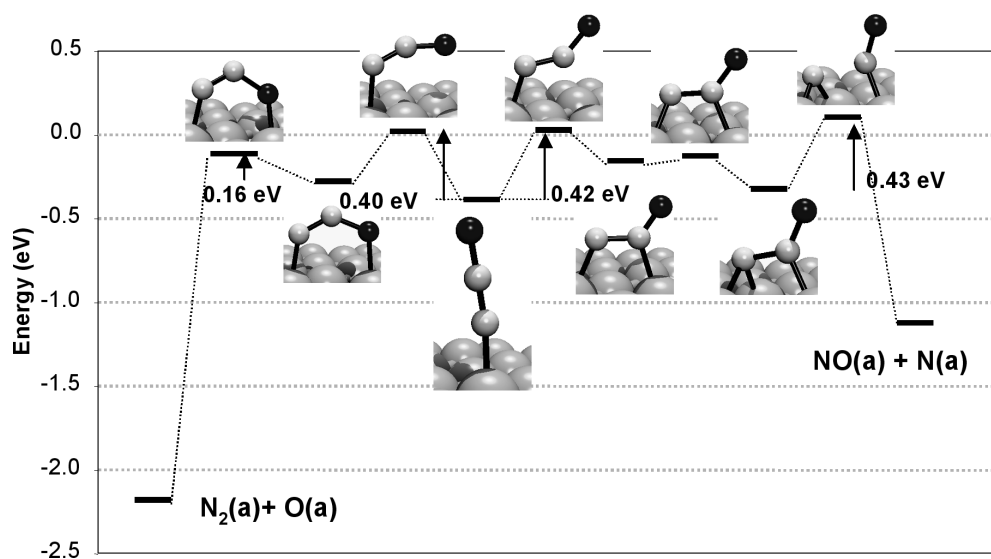


Fig. 6. Reaction paths for  $\text{N}_2\text{O}$  activation and decomposition into adsorbed  $\text{N}_2 + \text{O}$  and  $\text{NO} + \text{N}$ . The zero energy level corresponds to the non-interacting surface and  $\text{N}_2\text{O}$  in the gas phase.

the geometry in the gas phase. The angle  $\text{N-N-O}$  is  $128^\circ$  and the associated  $\text{N-O}$  (1.32 Å) and  $\text{N-N}$  (1.20 Å) distances are significantly larger compared with those in gas-phase  $\text{N}_2\text{O}$ . In this case the activation of the  $\text{N-O}$  bond is more important than the activation of the  $\text{N-N}$  bond, and this adsorption mode can be the starting point for the dissociation into  $\text{N}_2$  and  $\text{O}$  species. Therefore,  $\text{Rh}(111)$  can activate both the  $\text{N-N}$  and the  $\text{N-O}$  bonds of the  $\text{N}_2\text{O}$  molecule when flat, bidentate, adsorption modes are considered. Accordingly, the first step for  $\text{N}_2\text{O}$  decomposition should involve the transformation of the top adsorption mode into flat adsorption modes.

On oxide surfaces, the most stable adsorption mode is via the  $\text{O}$  atom, which leads to spontaneous  $\text{N}_2$  desorption. For  $\text{Rh}(111)$ , any attempt to start from  $\text{N}_2\text{O}$  adsorbed via  $\text{O}$  leads to desorption, and the direct transposition, characteristic of oxides, does not take place. In order to confidently exclude this possibility, we have computed the adsorption energy for  $\text{N}_2\text{O}$  adsorbed via  $\text{O}$  in top position for a fixed  $\text{Rh-O}$  distance. For  $\text{Rh-O}$  distances around 2.0 Å, the values of the  $\text{N-N}$  and  $\text{N-O}$  distances do not change with respect to the gas-phase molecule, and the adsorption energy is positive (0.4 eV for 2.13 Å and 0.6 eV for 2.03 Å, respectively). These results allow us to rule out this adsorption mode.

### 3.2.2. $\text{N}_2\text{O}$ dissociation

Starting from the more stable  $\text{N}_2\text{O}$  adsorption mode, two possible pathways stemming from  $\text{N}_2\text{O}$  dissociation have been modeled. The overall reaction path for  $\text{N}_2\text{O}$  decomposition on  $\text{Rh}(111)$  to give adsorbed  $\text{N}_2 + \text{O}$  or  $\text{NO} + \text{N}$  is shown schematically in Fig. 6, in which we have also displayed the transition states and intermediate adsorbate structures. Both processes are exothermic, particularly the path leading to  $\text{N}_2 + \text{O}$ . The activation energy is 0.4 eV, which is very similar to the barrier computed for  $\text{Pt}(111)$  [22].

Starting from the most stable  $\text{N}_2\text{O}$  adsorption mode, two transition states of about 0.4 eV must be overcome to originate adsorbed  $\text{NO} + \text{N}$ . Hence, both thermodynamically and kinetically, the favored decomposition process of  $\text{N}_2\text{O}$  corresponds to the formation of  $\text{N}_2$  and not that of  $\text{NO}$ . Since the adsorption energy of  $\text{N}_2$  on the surface is very low, it desorbs rapidly, leading to a high oxygen coverage on the surface, in agreement with experimental observations. On the other hand, the adsorption energy of  $\text{NO}$  ( $\sim -2.0$  eV) [45] is higher than the activation energy for  $\text{N}_2\text{O}$  formation.

Fig. 6 can also be used to explain the production of molecular nitrogen at relatively high temperatures in the reduction of  $\text{NO}$  by  $\text{CO}$  on  $\text{Rh}(111)$  via the formation and subsequent decomposition of an  $\text{N-NO}$  surface intermediate [27,28]. Although the present activation barrier for the reaction  $\text{NO}(\text{ads}) + \text{N}(\text{ads}) \rightarrow \text{N}_2\text{O}(\text{ads})$  on  $\text{Rh}(111)$  is relatively high (1.33 eV), it is lower than the theoretical value predicted by Burch et al. [20] of 1.78 eV. They ruled out this mechanism at low temperatures and speculated on the possibility of an alternative pathway involving a dimer ( $\text{NO}_2$ ) species. This possibility was also explored by Bogicevic and Hass [21] on  $\text{Cu}(111)$  and  $\text{Pt}(111)$ , who concluded that the dimer route is not possible on  $\text{Pt}(111)$ . In the present study, the computed activation barrier for the formation of  $\text{N}_2$  from adsorbed  $\text{N}$  atoms is 2.10 eV. Although these data have to be taken cautiously, since the interaction between co-adsorbed species is not considered and coverage effects may change the energy profile, it is reasonable to state that  $\text{N}_2\text{O}$  formation is preferred over  $\text{N}_2$  formation if both  $\text{NO}$  and  $\text{N}$  species are present on the surface. This supports the recent study [29] on the formation of  $\text{N}_2\text{O}$  and  $\text{N}_2$  in a steady-state  $\text{NO} + \text{CO}$  reaction on  $\text{Pd}(110)$ , which concluded that the pathway through the intermediate adsorbed  $\text{N}_2\text{O}$  prevails be-

low 600 K, whereas the associative desorption of nitrogen atoms dominates at higher temperatures.

The present results also provide theoretical support for a suggestion by Zaera and Gopinath [28], who stated that the most likely way for the undissociated NO to participate in molecular nitrogen formation is via the formation and subsequent decomposition of an N–NO surface intermediate.

#### 4. Conclusions

Density functional theory calculations elucidate molecular aspects of different catalytic processes involving N-containing species on Rh(111).

- It has been shown that CN formation from adsorbed C and N atoms is preferred over N<sub>2</sub> recombination. The formation of HCN via CH fragments reacting with adsorbed N atoms is energetically favored, supporting previous experimental findings.
- The processes of N<sub>2</sub>O dissociation into N<sub>2</sub> + O or NO + N are both exothermic on Rh(111), although the former is preferred thermodynamically. In addition, the energy barriers of the pathway toward adsorbed N<sub>2</sub> and O are slightly lower than those toward adsorbed NO + N. Therefore, it is concluded that N<sub>2</sub> is the main reaction product, in agreement with experimental results over Rh catalysts. Our results also support the conclusion that N<sub>2</sub>O can be formed as a reaction intermediate during the reduction of NO to N<sub>2</sub> over rhodium, by reaction between adsorbed NO and N atoms.

#### Acknowledgments

Funding from the Spanish Ministerio de Ciencia y Tecnología (BQU2002-04029-CO2-02), the Catalan government (2001SGR00315), the Netherlands Organization for Scientific Research (NWO), and CESCA-CEPBA (HPRI-1999-CT-00071) is acknowledged. Computer time was provided by the Centre de Recursos Informatique of the Lille University, the Centre de Supercomputació de Catalunya, and the Stichting Nationale Computerfaciliteiten (NCF).

#### References

- [1] G.A. Somorjai, Introduction to Surface Chemistry and Catalysis, Wiley, New York, 1994.
- [2] R.I. Masel, Principles of Adsorption and Reaction on Solid Surfaces, Wiley, New York, 1996.
- [3] F. Zaera, Prog. Surf. Sci. 69 (2001) 1.
- [4] R.A. van Santen, M. Neurock, Catal. Rev.-Sci. Eng. 37 (1995) 557.
- [5] R.A. van Santen, J.W. Niemantsverdriet, Chemical Kinetics and Catalysis, Plenum, New York, 1995.
- [6] R.D. Cortright, J.A. Dumesic, Adv. Catal. 46 (2001) 161.
- [7] A. Gross, Surf. Sci. 500 (2002) 347.
- [8] F. Illas, C. Sousa, J.R.B. Gomes, A. Clotet, J.M. Ricart, in: M.A. Chaer-Nascimento (Ed.), Theoretical Aspects of Heterogeneous Catalysis, Progress in Theoretical Chemistry and Physics, vol. 8, Kluwer Academic Publishers, Dordrecht, 2001, pp. 149–181.
- [9] C.J.H. Jacobsen, S. Dahl, B.S. Clausen, S. Bahn, A. Logadottir, J.K. Nørskov, J. Am. Chem. Soc. 123 (2001) 8404.
- [10] R.M. van Hardeveld, A.J.G.W. Schmidt, R.A. van Santen, J.W. Niemantsverdriet, J. Vac. Sci. Technol. A 15 (1997) 1642.
- [11] R.M. van Hardeveld, R.A. van Santen, J.W. Niemantsverdriet, J. Phys. Chem. B 101 (1997) 7901.
- [12] E. Herceg, M. Trenary, J. Am. Chem. Soc. 125 (2003) 15758.
- [13] F. Ample, J.M. Ricart, A. Clotet, D. Curulla, J.W. Niemantsverdriet, Chem. Phys. Lett. 385 (2004) 52.
- [14] N. Macleod, J. Isaac, R.M. Lambert, J. Catal. 193 (2000) 115.
- [15] F. Kapteijn, J. Rodríguez-Mirasol, J.A. Moulijn, Appl. Catal. B 9 (1996) 25.
- [16] J. Pérez-Ramírez, F. Kapteijn, G. Mul, X. Xu, J.A. Moulijn, Catal. Today 76 (2002) 55.
- [17] A. Kokalj, I. Kopal, H. Horino, Y. Ohno, T. Matsushima, Surf. Sci. 506 (2002) 196.
- [18] A. Kokalj, I. Kopal, T. Matsushima, J. Phys. Chem. B 107 (2003) 2741.
- [19] A. Kokalj, Surf. Sci. 213 (2003) 532.
- [20] R. Burch, S.T. Daniells, P. Hu, J. Chem. Phys. 117 (2002) 2902.
- [21] A. Bogicevic, K.C. Hass, Surf. Sci. 506 (2002) L237.
- [22] R. Burch, S.T. Daniells, J.P. Breen, P. Hu, J. Catal. 224 (2004) 252.
- [23] J.F. Paul, J. Pérez-Ramírez, F. Ample, J.M. Ricart, J. Phys. Chem. B 108 (2004) 17921.
- [24] V.P. Zhdanov, B. Kasemo, Surf. Sci. Rep. 29 (1997) 31.
- [25] D.N. Belton, C.L. DiMaggio, K.Y.S. Ng, J. Catal. 144 (1993) 273.
- [26] D.N. Belton, C.L. DiMaggio, S.J. Schmiege, K.Y.S. Ng, J. Catal. 157 (1995) 559.
- [27] F. Zaera, C.S. Gopinath, Chem. Phys. Lett. 332 (2000) 209.
- [28] F. Zaera, C.S. Gopinath, J. Mol. Catal. A 167 (2001) 23.
- [29] Y. Ma, I. Rzeznicka, T. Matshushima, Chem. Phys. Lett. 338 (2004) 201.
- [30] E.V. Kondratenko, J. Pérez-Ramírez, Catal. Lett. 91 (2003) 211.
- [31] G. Kresse, J. Hafner, Phys. Rev. B 47 (1993) 558.
- [32] G. Kresse, J. Hafner, Phys. Rev. B 48 (1993) 13115.
- [33] G. Kresse, J. Hafner, Phys. Rev. B 49 (1994) 14251.
- [34] J.P. Perdew, J.A. Chevary, S.H. Vosko, K.A. Jackson, M.R. Pederson, D.J. Singh, C. Fiolhais, Phys. Rev. B 46 (1992) 6671.
- [35] D. Vanderbilt, Phys. Rev. B 41 (1990) 7892.
- [36] H.J. Monkhorst, J.D. Pack, Phys. Rev. B 13 (1976) 5188.
- [37] G. Henkelman, B.P. Uberuaga, H. Jónsson, J. Chem. Phys. 113 (2000) 9901.
- [38] F. Ample, A. Clotet, J.M. Ricart, Surf. Sci. 448 (2004) 111.
- [39] W. Daum, F. Dederichs, J.E. Muller, Phys. Rev. Lett. 80 (1998) 766.
- [40] H. Yang, T. Caves, J.L. Whiten, J. Chem. Phys. 103 (1995) 8756.
- [41] G.L. Beltramo, T.E. Shubina, S.J. Mitchell, M.T.M. Koper, J. Electroanal. Chem. 563 (2004) 111.
- [42] A. Michaelides, P. Hu, J. Chem. Phys. 114 (2001) 5792.
- [43] A. Michaelides, Z.-P. Liu, C.J. Zhang, A. Alavi, D.A. King, P. Hu, J. Am. Chem. Soc. 125 (2003) 3704.
- [44] J.-L. Teffo, A. Chendin, J. Mol. Spectrosc. 138 (1989) 134.
- [45] D. Loffreda, D. Simon, P. Sautet, Chem. Phys. Lett. 291 (1998) 15.